

# Application News

Web Application Supporting Cellular Observations Cell Pocket™

## Morphological Analysis and Visualization of Morphological Changes in Cell Spheroids Using Deep Learning

Shuhei Yamamoto, Mika Okada, Toru Kaji, and Toru Ezure

### User Benefits

- ◆ Cell Pocket provides a simple means of quantifying sensuous observations.
- ◆ Quantified observation information can be used for objective evaluation of culture conditions.
- ◆ Objective assessment results can be shared with lab members along with data.

### Introduction

Human pluripotent stem cells are a heterogeneous population that change constantly during the culture process. The changing morphology of human pluripotent stem cells is considered an important quality characteristic, and evaluating product quality at the completion of manufacture, as is the case with small molecule drugs, is not a suitable approach for cell preparations. Given this backdrop, the industrialization of regenerative medicine and cell therapy requires methods of evaluating the status of cells that are noninvasive and provide observations over time.

A well-known noninvasive technique is the assessment of cell morphology by image analysis. Analyzing cell morphology once posed a significant challenge, but thanks to dramatic improvements in machine learning techniques and the increased availability of these techniques, cell morphological analysis is now feasible and attracting interest.

Shimadzu used segmentation by deep learning, a machine learning technique, to develop Cell Pocket, a web application that offers a simple platform for image analysis (Fig. 1). Cell Pocket is a user-friendly advanced image analysis tool that allows users to quantify their sensuous or experimental observations and derive important findings based on these observations. This article presents an example analysis that visualizes changes in spheroid morphology during the differentiation and maturation process of spheroids of endoderm cells derived from human iPSCs.

### Analytical Conditions

#### Cell Spheroids for Analysis

Some example images of the cell spheroid culture used in the analysis are shown in Fig. 2. The shape, pattern, color, and other morphological characteristics of the cell spheroids differ at each of the six differentiation stages.

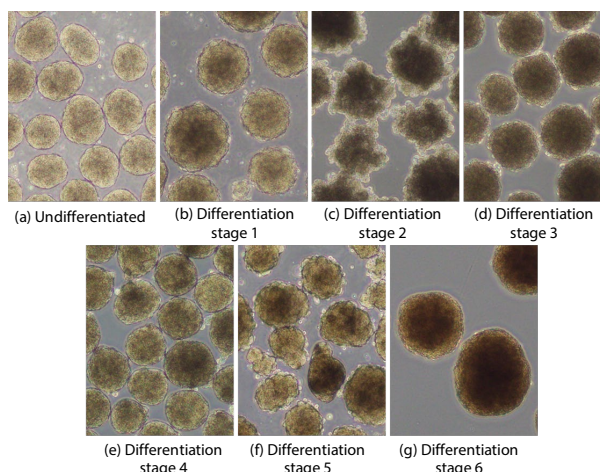


Fig. 2 Cell Spheroid Morphology at Each Differentiation Stage

The images used for analysis contained around 100 to 300 spheroids as shown in Fig. 3. Information about these images is shown in Table 1.

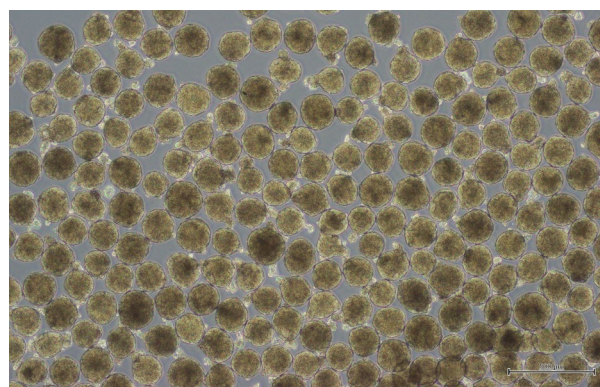
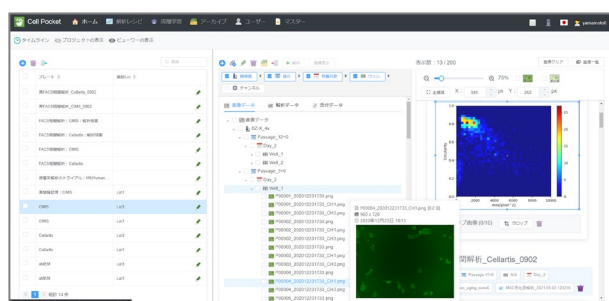


Fig. 3 Microscopic Image of Spheroids Used in Analysis



- Aggregate and accumulate laboratory data
- Analyze, view, and manage data even from the office

Fig. 1 Operation of Cell Pocket Web Application

Table 1 Image Information

Image Size:	1920 × 1440 pixels
Bit Depth:	24-bit (RGB)
File Format:	Portable Network Graphics (PNG)
No. of Analyzed Images:	14 images (2 of the undifferentiated state and 2 at each differentiation stage)

Learning Algorithm

Cell Pocket uses a deep-learning algorithm called semantic segmentation that attaches pre-learned labels to each pixel in an image.

For this analysis, the labels (1) spheroid, (2) spheroid perimeter, and (3) background were assigned to training images, as shown in Fig. 4, to create a trained model that recognized regions of an image as either label (1), (2), or (3). Images used to train in a trained model and identify regions are called target images, and images with labels are called labeled images. The labeled image data used in training is created by hand.

Once trained, the model is able to predict the regions of the image that represent spheroids, as shown in Fig. 5.

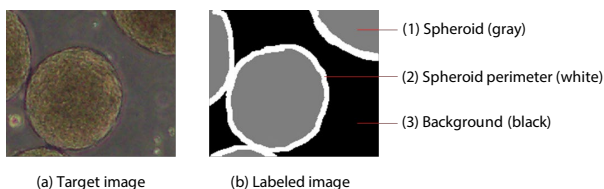


Fig. 4 Target Image and Labeled Image

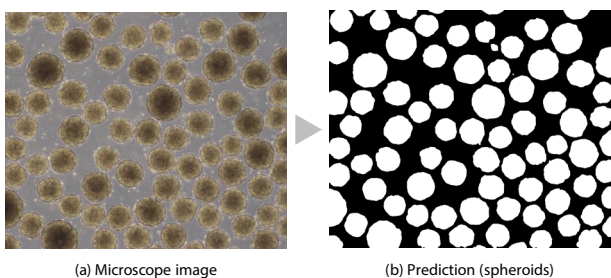


Fig. 5 Prediction by the Trained Model

Dataset

A dataset is the combination of target images and labeled images used to train a model and to evaluate the accuracy and performance of a trained model. A dataset contains three types of data: training data consisting of images used in training, validation data consisting of images used in training to evaluate model accuracy, and test data consisting of images used to evaluate the final performance of a trained model. Details of the dataset used in this example analysis are shown in Table 2. This dataset comprised the images for analysis shown in Table 1 and excerpted parts of images of cell spheroids cultured under similar culture conditions. Some examples from the dataset are shown in Fig. 6.

Table 2 Details of Dataset

Image Size:	197 × 165 pixels
Bit Depth:	24-bit (RGB)
File Format:	Portable Network Graphics (PNG)
No. of Images:	95 images (training: 60, validation: 22, test: 13)

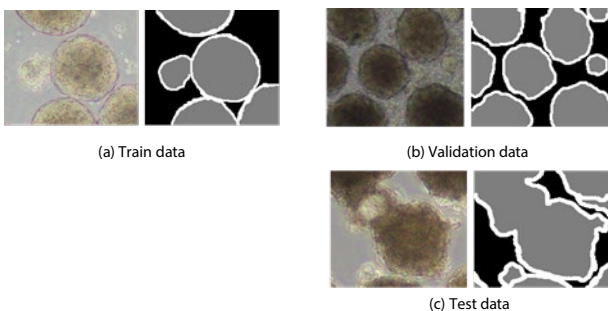


Fig. 6 Examples from Dataset

Trained Model Performance

The learning curve for the model is shown in Fig. 7. The horizontal axis of the learning curve shows the number of training iterations, and the vertical axis shows the error rate for training data and validation data and the loss function value. The red line is the loss function value, the blue line is the error rate for training data, and the green line is the error rate for validation data. The loss function is set to cross-entropy and the goal of training is to minimize the cross-entropy loss. As the number of training iterations increases, the loss function decreases and converges, while a similar tendency is seen in training data and validation data error rates, indicating the model is being trained successfully.



Fig. 7 Learning Curve

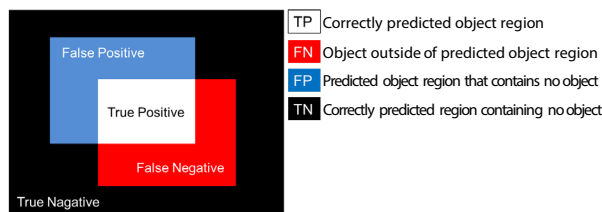
Table 3 shows the results of a performance assessment of the trained model using 13 test data images. The performance metrics in Table 3 are explained in more detail in Fig. 8.

An intersection over union (IoU) value of over 0.9 for spheroids indicates the model is accurate enough at identifying regions that represent spheroids. Fig. 9 shows spheroids identified by the trained model in an image from the test data set. In Fig. 9, regions identified as spheroids are shown as a blue overlay, and a blue perimeter is added when there is no contact with the edge of the image.

The model correctly identified the inner region (not including the perimeter) of the spheroids and removing the added spheroid perimeter shows the model identified touching spheroids as separate spheroids.

Table 3 Results from Performance Assessment of Trained Model

Performance Metric	Overall Mean	Background	Spheroid	Spheroid Perimeter
Accuracy:	0.954	-	-	-
IoU:	0.798	0.873	0.930	0.590
Precision:	0.874	0.922	0.959	0.742
Recall:	0.895	0.950	0.982	0.753



$$Accuracy = \frac{TP + TN}{ALL} \quad IoU = \frac{TP}{TP + FN + FP} \quad Recall = \frac{TP}{TP + FN} \quad Precision = \frac{TP}{TP + FP}$$

Fig. 9 Explanation of Performance Metrics

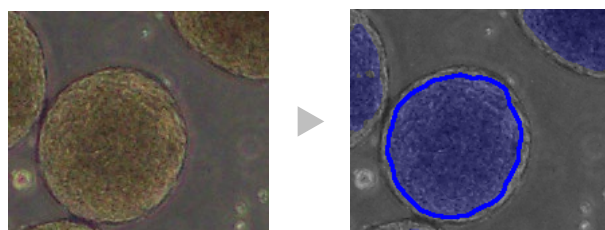


Fig. 9 Spheroids Predicted by Trained Model in Test Data



## ■ Analysis Method

Cell Pocket allows the user to register an analysis method, called an “analysis recipe,” that combines the trained model with various analytical processes that include image processing. The analysis method shown in Fig. 10 was created to visualize the distribution of spheroid area and circularity.

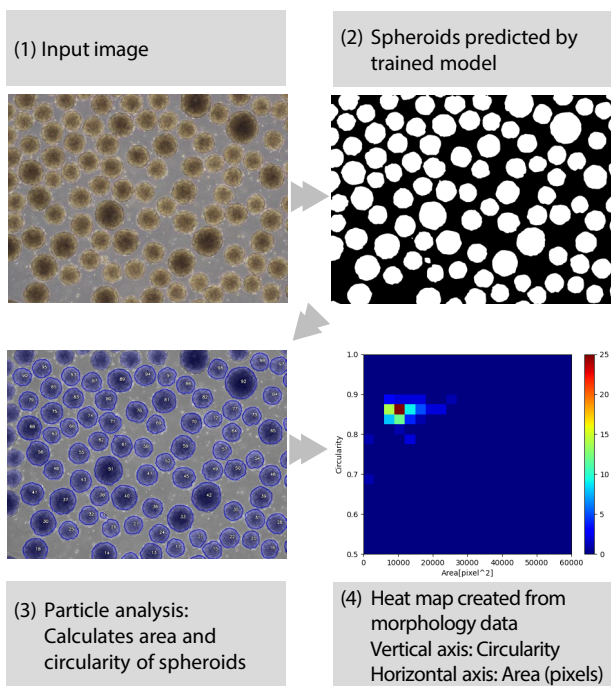


Fig. 10 Analysis Method

In addition to area and circularity, particle analysis can be used to obtain information such as perimeter length; bounding rectangle major axis length, minor axis length, aspect ratio, and angle; mean luminance and luminance variation; and tone.

Using the index of “Ambient length, aspect ratio of circumscribed rectangle, average and variance of brightness, color” which is the result of particle analysis of each differentiation stage, dimensional compression was performed by the t-SNE method to investigate whether there were morphological differences of spheroids at each differentiation stage.

## ■ Results

Using particle analysis, the distribution of spheroid area and circularity at each differentiation stage was visualized in heat maps (Fig. 11). The heat maps show that spheroids of undifferentiated cells were uniform in area ( $\approx$  size) and circularity, whereas spheroid circularity varied greatly at differentiation stages 2 and 5. The heat maps also show that some spheroids with low circularity emerged at differentiation stages 1 and 4 prior to differentiation stages 2 and 5. Conversely, the spheroids at differentiation stage 3 are uniform in area and circularity. This method of visualizing changes in spheroid morphology can be used to identify unexpected morphological changes in real-time.

Fig. 12 shows results from a t-SNE-based dimensional compression of morphological data for individual spheroids. Each spheroid of each differentiation stage was colored, confirming that clusters were formed in each undifferentiated state or differentiation stage.

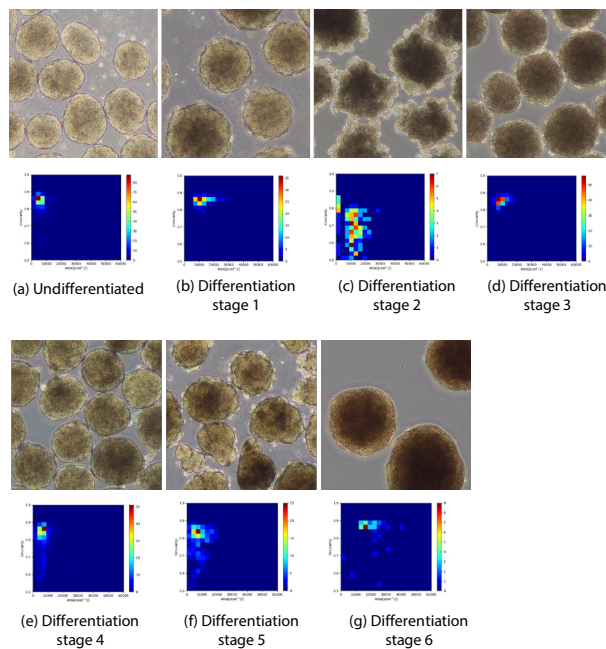


Fig. 11 Distribution of Cell Spheroid Area and Circularity at Each Differentiation Stage

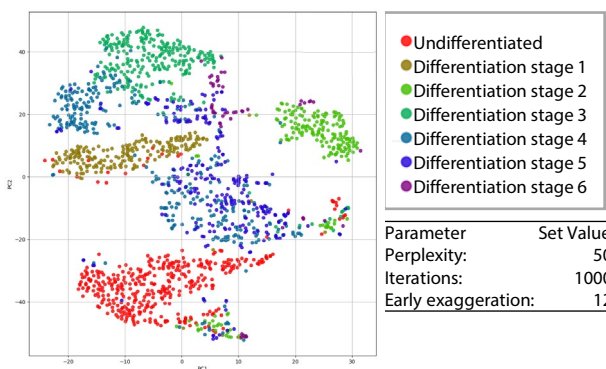


Fig. 12 Dimensional Compression of Morphological Data by t-SNE

## ■ Conclusion

Cell Pocket was used to perform a morphological analysis on human iPSC spheroids undergoing pancreatic differentiation. Training data was created from parts of images and a trained model was created that could identify spheroids. The morphological information of each spheroid was extracted by performing particle analysis on the spheroid area estimated by the trained model. Heat maps showing the distribution of these morphological metrics at each stage of differentiation were used to visualize how these metrics change during culture. Applying dimensional compression by t-SNE to these morphological information also revealed clusters corresponding to each stage of differentiation. These findings from morphological analysis offer an effective and noninvasive means of evaluating the status of cell cultures.

Lastly, we would like to thank Professor Shoen Kume and Associate Professor Nobuaki Shiraki of the Kume & Shiraki Laboratory, Tokyo Institute of Technology, for providing the image data analyzed in this article and their valuable comments on the results.

Cell Pocket is a trademark of Shimadzu Corporation and/or its affiliates in Japan and other countries.



Shimadzu Corporation

www.shimadzu.com/an/

**For Research Use Only. Not for use in diagnostic procedures.**

This publication may contain references to products that are not available in your country. Please contact us to check the availability of these products in your country.

The content of this publication shall not be reproduced, altered or sold for any commercial purpose without the written approval of Shimadzu. See <http://www.shimadzu.com/about/trademarks/index.html> for details.

Third party trademarks and trade names may be used in this publication to refer to either the entities or their products/services, whether or not they are used with trademark symbol “TM” or “®”.

Shimadzu disclaims any proprietary interest in trademarks and trade names other than its own.

The information contained herein is provided to you “as is” without warranty of any kind including without limitation warranties as to its accuracy or completeness. Shimadzu does not assume any responsibility or liability for any damage, whether direct or indirect, relating to the use of this publication. This publication is based upon the information available to Shimadzu on or before the date of publication, and subject to change without notice.